Turk J Chem
35 (2011) , 225 – 235.

doi:10.3906/kim-1007-758

Stability study of passive film on copper surface as a function of anodic potential

Amtul NASEER[1,*], **Athar Yaseen KHAN**[2]
[1] *Chemistry Department, Quaid-i-Azam University, Islamabad-PAKISTAN*
[2] *Chemistry Department, Allama Iqbal Open University, Sector H-8, Islamabad-PAKISTAN*
e-mail: hanm_7@yahoo.com

Received 07.07.2010

Results for passive film formation and breakdown on copper disk electrodes in buffer solutions, pH 9.2 and 8.5, were reported earlier. The present studies were carried out in a buffer solution, pH 8.0, and together these studies make good material for understanding the effect of pH changes on film texture as a function of potential. Cyclic voltammetry (CV) and electrochemical impedance spectroscopy (EIS) were used to examine passive film and the variations it went through upon being treated potentiostatically in the range of -0.3 to 0.9 V. On the basis of equivalent circuits used for modeling impedance data in this potential range, 4 stages were identified. The proposed circuits for different potential ranges illustrated the Cu/oxide/electrolyte systems and their properties in terms of 2 interfaces. A criterion for the applicability of the equivalent circuit model was discussed. Changes in the film-metal interface as a function of potential were also probed at 30 mHz with Nyquist plots. Diffusion coefficients for ionic movement at 4 potential values in the film, calculated from the EIS data, were of the order of 10^{-5} cm^2 s^{-1}.

Key Words: Electrochemical impedance spectroscopy, model circuits, copper surface, passive film, transition stage, interfaces, diffusion coefficient

Introduction

Corrosion of copper occurs in the presence of oxygen when it is in contact with electrolytes. The oxide layer has, in general, a duplex structure made up of an inner Cu_2O barrier layer, followed by $CuO/Cu(OH)_2$.[1] The quantity and nature of the constituent oxides/hydroxides in passive film formed over a copper surface strongly depend upon the pH of the solution, the potential of formation, and the temperature. Feng et al.[2] and Laz et

*Corresponding author

al.[3] showed the strong reliance of film texture on the pH of the solution. It was reported earlier that passive film stability showed a relationship between the pH of the formation and applied potential.[4,5]

The importance of film formation has attracted considerable interest in many areas of research to study the phenomena of corrosion, electrocatalysis, and double-layer structures.[6] However, the inherent complexity of the system still leads to the emergence of problems that keep the future research doors open. To develop a deep understanding of passivity growth and breakdown requires knowledge of minor details at the atomic level. A study of the changes that take place during this process as imposed potential progresses anodically in a particular buffer solution provides one such approach. A prerequisite for such studies is an in situ technique.

Different techniques offer various limitations, whereas electrochemical impedance spectroscopy (EIS) is a powerful, nondestructive, and surface state-sensitive technique. It makes measurements possible with almost no loss in the weight of the sample, an important requirement for corrosion and passive layer studies. Moreover, fitting of impedance data to circuits and the use of a constant phase element (CPE) has further facilitated the analysis of the surface to explore the mechanism of ionic movement in passive layers. Very few papers have been devoted to the study of copper passivity using EIS alone.

Earlier studies to investigate the texture of passive film in buffer solutions of pH 9.2 and 8.5 have been carried out. The present study is an extension of the work previously reported[4,5] and is specifically focused on investigating changes that took place in passive film growth and its transpassivity region as the pH was lowered to 8.0. EIS was employed as the main technique with anodic potential imposed in a stepwise fashion.

Experimental

The details of the copper disk electrode construction and the cleaning of its surface have already been described.[4]

Triply distilled water was used to prepare a buffer solution of pH 8.0 by mixing solutions of NaH_2PO_4 and Na_2HPO_4 (BDH AnalaR grade) of requisite concentrations, and the hydrogen ion concentration was monitored with a pH meter from Horiba (Japan). A standard 3-electrode cell was used for electrochemical measurements. The electrode was pretreated at -1.4 V for 45 s using a PAR 173 potentiostat/galvanostat for removal of impurities. A cyclic voltammogram was recorded at a scan rate of 50 mV s^{-1} in the range of -1.2 to 1.0 V with a spirally coiled platinum wire as the counter electrode. All potentials in this work were referred to a saturated calomel electrode (SCE).

Impedance data at ambient temperature, in the frequency range of 30 mHz-100 kHz, were collected using a 3-electrode system on a TFA 2000 impedance analyzer from Sycopel Scientific (UK). The interfering circuit of the reference electrode was removed by connecting a platinum wire electrode serving as a sonde via a 10 μF capacitor. The strength of the perturbation potential used in all measurements was 5 mV peak-to-peak. Prior to measurement at each potential, the sample disk was potentiostatically polarized to the desired potential for 10 min.

Results and discussion

Cyclic voltammogram (CV) of copper surface

Cyclic voltammetry provided information about oxide formation on the metallic electrode surface (Figure

1).[6] According to Pourbaix,[7] the following redox reactions were expected to take place in an aqueous electrolyte at pH 8.0:

$$2Cu + H_2O = Cu_2O + 2H^+ + 2e^-; E = -0.243V/SCE \quad (1)$$

$$Cu + H_2O = CuO + 2H^+ + 2e^-; E = -0.145V/SCE \quad (2)$$

$$Cu + 2H_2O = Cu(OH)_2 + 2H^+ + 2e^-; E = -0.105V/SCE \quad (3)$$

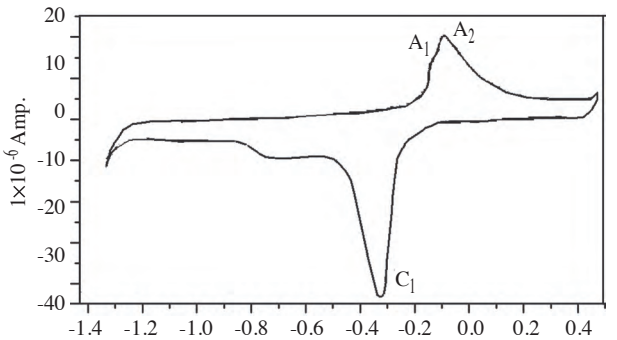

Figure 1. Cyclic voltammogram of copper in buffer solution of pH 8.0 at a scan rate of 50 mV s^{-1}.

The peak resolution appeared to be strongly scan rate-dependent when tested with other pH buffer solutions;[8] however, in this system, it exhibited independence. A prominent shoulder with 2 peaks was observed at a scan rate of 50 mV s^{-1}. Contrarily, Laz et al. reported 2 peaks at a scan rate of 10 mV s^{-1}.[3] Apparently surface contamination, along with differing methods of preparation, affects the number of peaks in CVs.[9] In the experiment carried out, the drag particular to CV shifted the peak values as compared to the potentials predicted by Pourbaix. Appearance of a shoulder, A_1, signified the reaction represented in Eq. (1), instantly followed by a broad peak, A_2, highlighting the combination of the reactions represented by Eqs. (2) and (3) (Figure 1).

As expected, the reactions continued along with the anodic potential progression. A broad cathodic peak due to lack of resolution and CV drag around -0.33 V was hypothesized as the combination of reverse reactions given by Eqs. (1), (2), and (3). The high current value during the reverse scan indicated a large amount of copper ions going back into copper. Detailed information regarding the nature of the ionic movement leading to passivity breakdown at specific potential values was later extracted from EIS.

EIS studies of copper surface

Impedance characteristics of freshly prepared copper electrode in the frequency space of 30 mHz-100 kHz, powered by an AC signal of 5 mV peak-to-peak, were employed in this study. The electrode was subjected to static potential from -0.3 to 0.9 V and the progression in the potential regime was in steps of 0.1 V. Impedance data were fitted through the EQUIVCRT program,[10] which made use of some elements as calculation variables.[11]

Based on the circuits used in fitting results, the entire potential range for studying the passive film was divided into 4 stages, in contrast to the passive film in buffer solutions of pH 9.2 and 8.5.[4,5] These stages

were: the initial stage of oxide growth, from -0.3 to -0.2 V; the middle stage, structural changes, from -0.1 to 0.2 V; the transition stage, 0.3 V; and the final stage, the transpassivity region, 0.4-0.9 V. Equilibrium redox potentials for the formation of Cu_2O from copper and CuO and $Cu(OH)_2$ from Cu_2O (Eqs. (1) to (3)) showed that in the first potential region, the formation and growth of the inner layer of Cu_2O occurred as in Figure 2. The capacitive circuit (Figure 3, inset), which characterized a diffusion process, represented the behavior of the modified film. In the third potential stage, complete removal of the passive film occurred, and in the final stage, the charge transfer process set in specifically at 0.4 and 0.7 V.

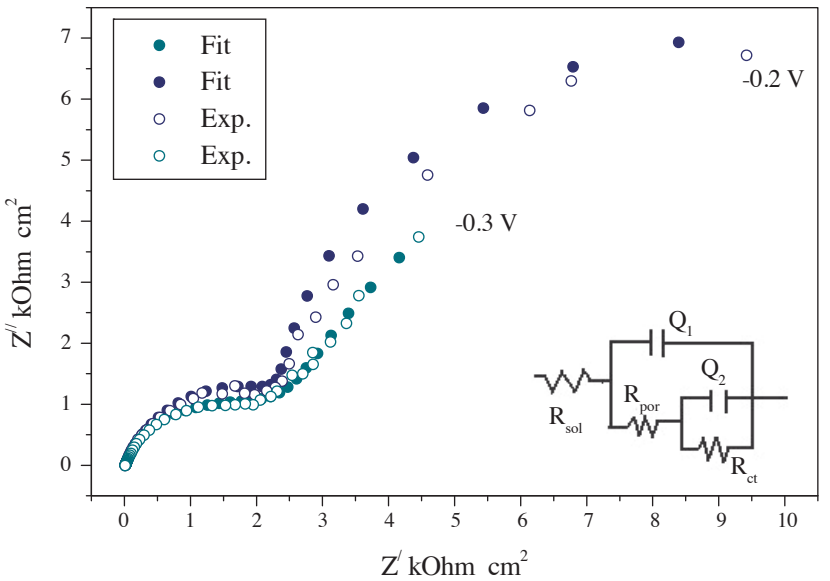

Figure 2. Nyquist plots and the circuit used to fit the impedance data for initial stage of passivation of copper surface.

It should be pointed out that EIS is a potentiostatic technique, and prior to EIS measurements at each potential step, the electrode was given sufficient time for stabilization.

Initial stage

In this stage, collection of impedance data was reduced to 2 voltage steps, in comparison to 5 and 4 voltage steps in buffer solutions of pH 9.2 and 8.5. Furthermore, this stage required an entirely different interpretation for the passive films.[4,5] In a buffer solution of pH 8, the first step at -0.3 V was the preparatory step in oxide formation, and -0.2 V was where Cu_2O was formed (Eq. 1), leading to passive layer formation over the copper surface.

Normalized Nyquist plots with Z' and Z'' (Figure 2) indicated the presence of 2 time constants, a high frequency incomplete semicircle and a low frequency rising arc. This was verified by the electrical equivalent circuit (EEC) model (Figure 2, inset) used to fit the experimental data. The high frequency time constant included R_{por} and Q_1, where R_{por} is the resistance of the pores present in the passive layer and Q_1 represents the double-layer capacitance at the oxide-electrolyte interface. The low frequency time constant is a parallel combination of R_{ct}, the charge transfer resistance, and Q_2, the capacitance at the oxide-metal interface. Theoretical and experimental results showed good agreement by the inclusion of frequency dependent CPEs,

here represented by Q_1 and Q_2. The impedance of CPE is defined by:[12]

$$Z_{CPE} = [Q(j\omega)^n]^{-1}. \tag{4}$$

The decrease in Q_1 at -0.2 V with potential indicated that the adsorbed OH^- ions at -0.3 V reacted with copper, thus reducing the charge, while n_1 persisted. The resistance R_{por} increased with potential at -0.2 V due to more porous film formation. R_{por} values indicated surface coverage of metal by Cu^{1+} that offered hindrance for the movement of OH^- ions, as also confirmed by R_{ct}. The Q_2 value was quite high at -0.3 V owing to adsorption[13] and decreased by more than 50% at -0.2 V. Selective oxide film formation at -0.3 V appeared likely on the electrode surface, giving roughness to the surface with an n_2 value of 0.83, while the reaction at -0.2 V increased the n_2 value, homogenizing the surface.

The inclusion of 2 time constants was justified as, mathematically, the circuit used to fit the impedance data satisfied the criteria given in Eqs. (5) and (6); the separation of 2 time constants seems plausible[14] if:

$$0.2 < R_{ct}/R_{por} < 5 \tag{5}$$

and

$$0.05 > \tau_t/\tau_p > 20. \tag{6}$$

Consequently, the low frequency phenomenon could be studied independently of the high frequency phenomenon. Objectively, the ratio of R_{ct} to R_{por} was 5.3 for the potential value of -0.3 V and 3.4 for -0.2 V, while $\tau_t/\tau_p = 65.6$ for -0.3 V and 21 for -0.2 V. Here, τ_t is the time constant at the lower frequency and τ_p is the time constant at the higher frequency. As the semicircles were not complete, a curved line was obtained at the low frequency end; therefore, the nonideal Warburg impedance, Z_w, appeared to be involved in the spectrum. In the classical manner, it is written as:[14]

$$Z_w = (\sigma\omega^{-0.5} - j\sigma\omega^{-0.5}), \tag{7}$$

where σ = constant, $\omega = 2\pi f$, and f = frequency (Hz).

The presence of Z_w produced a diffusion tail in the complex plane plot that inclined exactly at 45° to the real axis.

For an AC diffusion layer thickness less than the DC Nernstian diffusion layer thickness, Eq. (7) results and is modified for equal AC and DC diffusion layer thicknesses as follows:[15]

$$Z_w = \sigma\omega^{-0.5}\tanh(\delta(j\omega/D)^{0.5}), \tag{8}$$

where δ = the diffusion layer thickness and D = the diffusion coefficient.

The nature of the system is strongly determined by the numerical values of $(\delta/(D)^{0.5})$. The tanh term could be approximate to unity at the lowest frequency with $\delta/(D)^{0.5} > 5$ so that Eq. (8) acquires the form of Eq. (7) and a 45° diffusion tail results, or the increased significance of the tanh term could result in the reversed condition. The type of kinetics that are rate controlling can be predicted by the predominant shape of the complex plane plot. The dominance of the diffusion process can be observed when:[14]

$$\sigma/R_{ct} \leq 0.1. \tag{9}$$

A semicircle will predominate, indicating that charge transfer is occurring at a slow rate. For the opposite case, if the diffusion tail interacts with a semicircle, $\sigma/\mathrm{R}_{ct} > 50$ (approx.), the diffusion process would occur more slowly than the charge transfer reaction. The low frequency regions of the complex plane plot were used to approximate the value of σ, using the imaginary part of Eq. (7):

$$Z'' = \sigma\omega^{-0.5}. \tag{10}$$

From the present experimental data, $\sigma/\mathrm{R}_{ct} = 0.043$ at the anodic potential value of -0.3 V. This value indicates that charge transfer took place at a faster pace than the diffusion process, suggesting the chemical adsorption of ions. Similarly, for -0.2 V, the value of $\sigma/\mathrm{R}_{ct} = 0.087$ approached Eq. (9), proving that the charge transfer reaction further validated the $\mathrm{Cu_2O}$ formation as in Eq. (1).

Second stage

Changes in the oxides' film as a result of potential increase were made apparent by varying shapes of Nyquist plots (Figure 3). The potential range for this stage extended cathodically in comparison to the potential range for the films formed at pH 9.2 and 8.5.[4,5] From -0.1 to 0.2 V, a gradual decrease in the Z′ and Z″ values was observed. This shape is characteristic of the diffusion-controlled process responsible for the ionic propulsion into the solution.

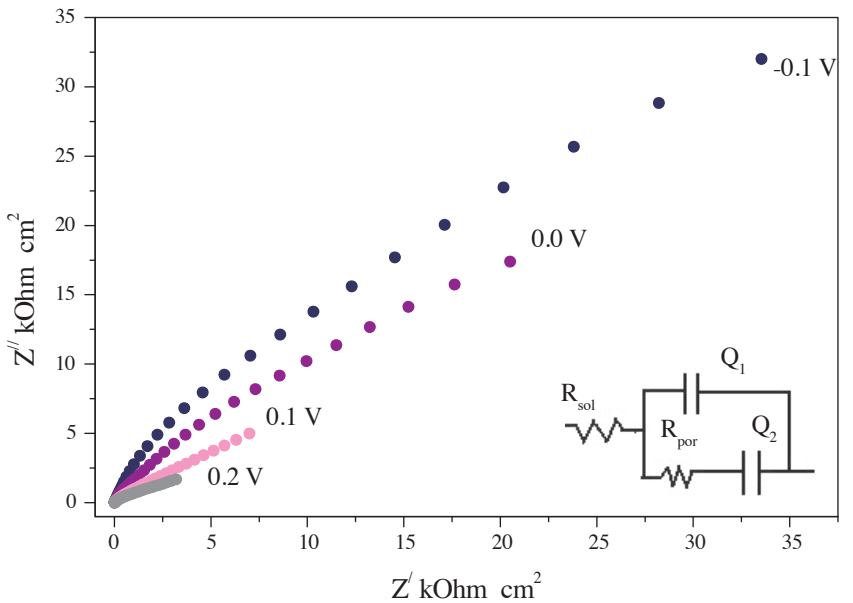

Figure 3. Nyquist plots and the circuit used to fit the impedance data for second stage of passivation of copper surface.

The impedance data were best fitted to capacitive circuit topology (Figure 3, inset) when the charge transfer was masked by diffusion. The film resistance (R_{por}) dropped from its largest value of 27.1 kΩ cm^2 at -0.1 V to 0.55 kΩ cm^2 as the potential increased to 0.2 V. This indicated the stability of the barrier layer at -0.1 V, followed by a dissolution process in the film leading to a decreased R_{por} (Table 1). The diffusion of species caused the depletion of oxide/hydroxide in the film. The average value of Q_1 in this potential region

was 65.2 Ω^{-1} cm^{-2} s$^{0.5}$. The dissolution of the film was accompanied by decreased n_1 values, indicating increased surface roughness. Q_2 values suggested that the film was overwhelmed with adsorbed species due to the strong affinity of copper for oxygen in this potential region, as also suggested by SERS studies.[13] The solid phase of the film mixed with the electrolyte and n_2 reflected this. The impedance spectrum shaped into a curve, showing that the film was removed from the surface and another reaction was likely to proceed over it.

Table 1. EIS best fit results of copper surface at varying potentials.

Potential in V	$Q_1\times 10^{-6}$ Ω^{-1} cm^{-2} s^n	n_1	R_{por} k Ω cm^2	R_{ct} k Ω cm^2	$Q_2\times 10^{-6}$ Ω^{-1} cm^{-2} s^n	n_2
-0.3	73.7	0.78	2.78	12.3	908	0.83
-0.2	65.8	0.78	3.60	14.8	414	1.00
-0.1	51.6	0.82	27.1	-	54.9	0.48
0.0	50.6	0.75	12.3	-	73.5	0.45
0.1	91.0	0.66	5.02	-	348	0.60
0.2	67.6	0.73	0.550	-	434	0.30
0.3	33.3	0.88	-	6.14	276	0.30
0.4	86.7	0.89	0.46	5.57	321	0.60
0.5	138	0.86	0.78	26.6	236	0.71
0.6	139	0.87	0.56	36.7	168	0.78
0.7	194	0.96	0.46	47.0	166	0.82
0.8	187	0.82	0.59	45.2	79.8	0.88
0.9	201	0.92	0.08	11.5	227	0.80

At -0.1 V potential, the electrode surface was mostly covered with the oxide layer. The diffusion of ions from the oxide layer superseded the charge transfer process. The effect of the potential on the film-solution interface could be discussed using the kinetic parameter characterizing the diffusion coefficient of Cu^{x+} (x = 1, 2) ions by:[16]

$$S = RT/n^2F^2c\sqrt{2D}; S = 1/Q\sqrt{2}. \tag{11}$$

Table 2 shows that the numerical values of diffusion coefficients gradually increased with potential. Furthermore, a comparison of the order of magnitude of the diffusion coefficient in buffer solutions with pH 9.2 and 8.0 clearly indicates the textural differences of the passive films formed in the 2 media. Movement of ions in the solid phase is the rigorous conclusion drawn for passive film formed in a buffer solution of pH 9.2,[4] and the solution phase for passive film formed in buffer solution with a pH of 8.0 indicated the loose passive film structure. Rapid removal of passive film is the ultimate outcome in the latter case. A possible explanation for the growth of film and depletion by the diffusion phenomenon can be taken from the point defect model.[17,18] According to this model, the oxidation of metal atoms to form ions at the metal-oxide (inner) interface generates a deriving force to form anion vacancies.

$$Cu_{Cu}(m) = Cu_{Cu}(ox) + 1/2V_o^{\cdot\cdot}(ox) + e, \tag{12}$$

where $Cu_{Cu}(m)$ is a copper atom in a regular metal site, $Cu_{Cu}(ox)$ is a copper cation in a regular site of the oxide film, $V_o^{\cdot\cdot}$ is a positively charged oxygen vacancy, and e represents the electron. At the oxide-electrolyte (outer) interface anion, vacancies become occupied by anions:

$$V_o^{\cdot\cdot}(ox) + H_2O(aq) = O_o(ox) + 2H^+(aq), \tag{13}$$

where $O_o(ox)$ is an oxygen anion in a regular site of the oxide film and H^+(aq) is the hydrogen ion in the aqueous electrolyte. Cation vacancies, formed by dissolution of cations into the electrolyte diffused toward the inner interface, can be represented as:

$$Cu_{Cu}(ox) = Cu^{x+}(aq) + V'_{Cu}(ox), \tag{14}$$

which could be exchanged with cations:

$$Cu_{Cu}(m) + V'_{Cu}(m) = Cu_{Cu}(ox) + V_{Cu}(m) + e. \tag{15}$$

Table 2. Diffusion coefficient of ions of passive film as a function of potential.

Potential V^{-1}	D $\times$ 10^{-5} cm^2 s^{-1}
-0.1	1.33
0.0	2.42
0.1	53.4
0.2	83.2

Here, $Cu^{x+}(aq)$ is a positively charged copper cation in the aqueous electrolyte, $V'_{Cu}(ox)$ is a negatively charged cation vacancy in the oxide, $V'_{Cu}(m)$ is a negatively charged vacancy at the metal surface, and $V_{Cu}(m)$ is a neutral vacancy in a regular metal site.

$$Cu_{Cu}(ox) = Cu^{x+}_{solution} + V''_{Cu}(ox), \tag{16}$$

where $Cu^{x+}_{solution}$ is the ion that moves into the solution and $V''_{Cu}(ox)$ is the vacancy created in the passive layer. The anodic potential increases, quickly deriving ions and leading to metal dissolution.

Transition stage

Figure 4 shows the experimental data and model circuit for the copper surface at 0.3 V. Only the low frequency time constant, with a parallel arrangement of elements, clearly indicated a charge transfer process starting at 0.3 V. The absence of R_{por} suggested an oxide layer removal. In accordance with the point defect model, at this and higher potentials, ions were removed from the film and the metal surface was exposed to the environment, where the charge transfer reaction/process could reoccur. The metal-film interface was the source of oxide ion vacancies and the film-solution interface was the pool for the same vacancies. The net result was oxide growth when the oxide vacancy diffused in and metal ions dissolved out of the solution.[17,18]

The lack of a transition stage in fitting results of passive film formed in buffer solutions of pH 9.2 and 8.5 added to its stability. Q_1 reflected the small charge accumulation at the oxide-electrolyte interface. However, the R_{ct} and Q_2 values indicated that a charge transfer reaction had started (Table 1).

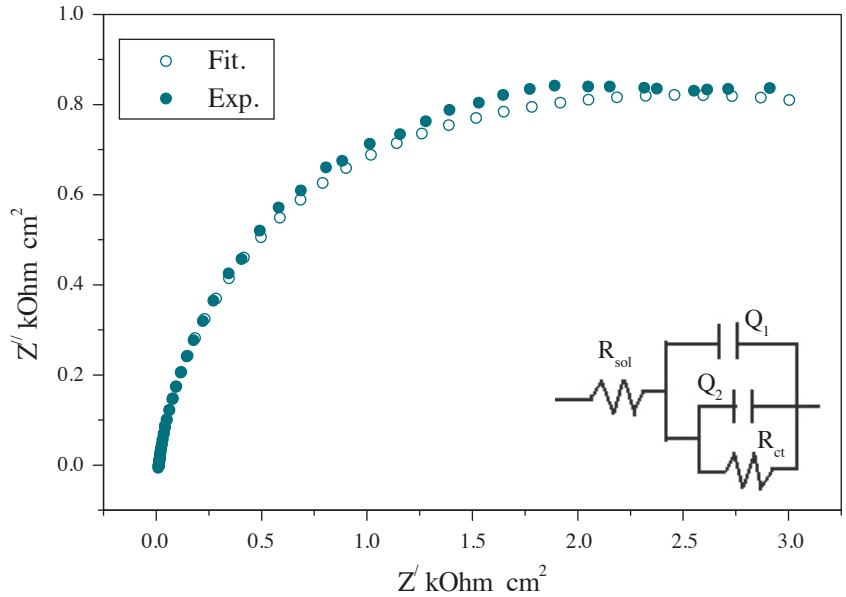

Figure 4. Nyquist plots and the circuit used to fit the impedance data for transition stage.

Final stage

Similar to the final stages of passive films studied earlier, this stage consisted of 6 potential steps, as shown in the Nyquist plots of Figure 5. The reaction of the surface with the environment at 0.4 V indicated a charge transfer reaction with the already used surface to form new products.

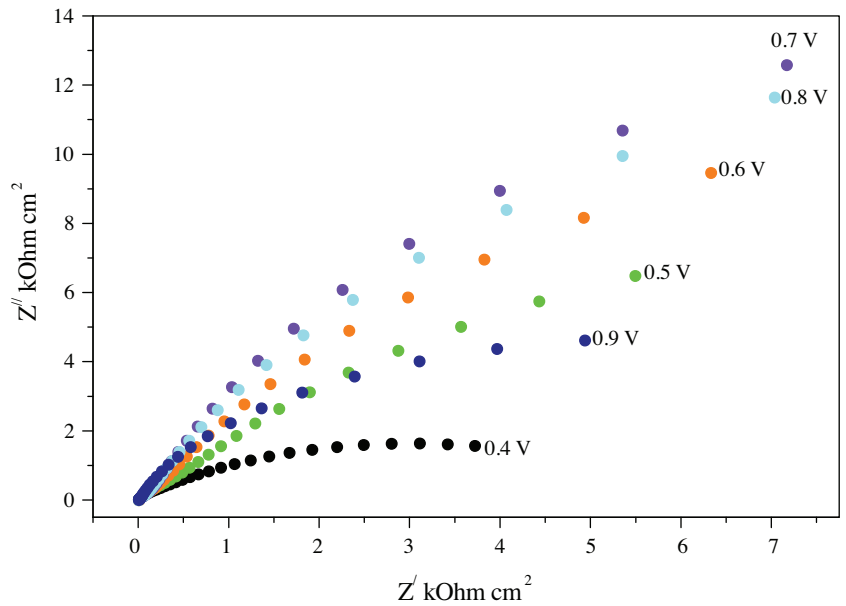

Figure 5. Nyquist plots for final stage of passivation of copper surface.

The fitting results presented in Table 1 were obtained by using the circuit shown in the inset of Figure 2. The effect of potential was clear as R_{ct} kept increasing from 0.4 to 0.7 V. Oxide film built up at previous potentials and continued at a slowed pace at higher potentials, finally becoming stable in the region of 0.7 V. A decrease in Q_2 values was observed as the potential progressed, while increased surface homogeneity was suggested by increasing n_2 values. At 0.9 V, lower R_{ct} and higher Q_2 values suggested the approach of the oxygen evolution limit, i.e. the transpassivity region.

R_{por} values remained in the range of 0.5-0.8 kΩ cm^2 and n_1 values also did not show marked change, except at 0.9 V. The low R_{por} values suggested that the newly formed film was not thick and/or that the surface was covered unevenly, in contrast to the R_{por} values observed in buffer solutions of higher pH values. Q_1 values also indicated some dissolution process accompanied with charge accumulation at the interface, since the solution was unstirred.

Data analysis at 30 mHz frequency

Figure 6 shows variation in Z' and capacitance measured at 30 mHz with potential. Regions of marked variation in Z' and Z'' were -0.3 to 0.1 V and 0.1 V to 0.5 V, respectively. This trend indicated a clear difference of the oxide behavior at the outset of formation and afterwards. The adsorption of charged species at 0.3 V validated the film removal and reoccurrence of reactions. Real (Z') and imaginary (Z'') values measured at 30 mHz decreased as potential increased, indicating that the film softened and was retained at the surface, accumulating more charge. The passive film structure formed in a buffer solution of pH 8.0 was totally different from that formed in buffer solutions of pH 9.2 and 8.5.

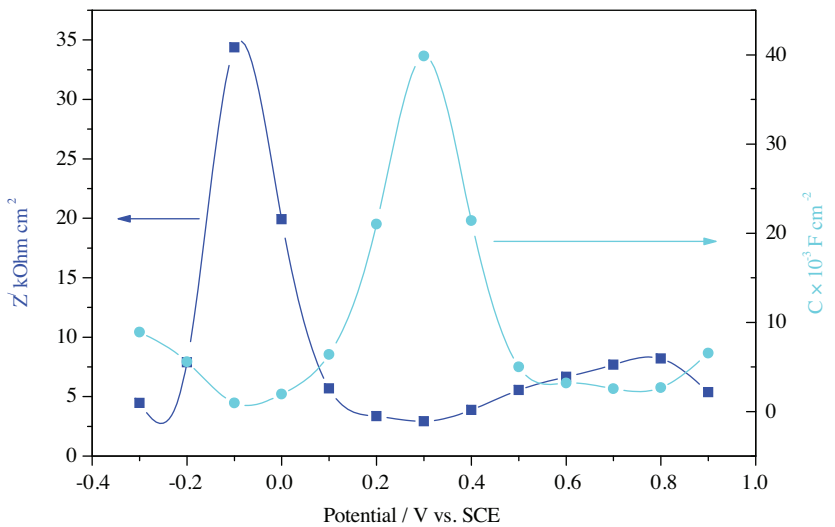

Figure 6. Variation of Z' and capacitance, C versus potential at 0.03 Hz.

Conclusion

Compared with oxide layers formed in buffer solutions with pH values of 9.2 and 8.5, film formation and stability were found to be steadily affected in a buffer solution of pH 8.0, as 2 potential steps were included in

the initial stage. While the second stage was spread over 4 potential steps, it was mainly active for the diffusion phenomenon. The diffusion of ionic species from the passive film started at -0.1 V and accelerated up to 0.2 V, finally resulting in its total removal at 0.3 V. Lack of a continuous passive film was suggested by simultaneous formations and removal of copper oxides/hydroxide in an irregular fashion on the surface during final stage.

Acknowledgment

The authors are greatly obliged to Harisah Mehmood for providing technical assistance during the write-up of the manuscript.

References

1. Babic, R.; Metikos-Hukovic, M.; Jukie, A. *J. Electrochem. Soc.* **2001**, *148*, B146-B151.
2. Feng, Y.; Siow, K.-S.; Teo, W.-K.; Tan, K.-L.; Hseih, A.-K. *Corrosion (Houston)* **1997**, *53*, 389-398.
3. Laz, M. M.; Souto, R. M.; Gonzalez, S.; Salvarezza, R. C.; Arvia, A. J. *Electrochim. Acta* **1992**, *37*, 655-663.
4. Naseer, A.; Khan, A. Y. *Turk. J. Chem.* **2009**, *33*, 739-750.
5. Naseer, A.; Khan, A. Y. *Turk. J. Chem.* **2010**, *34*, 815-824.
6. Kautek, W.; Gordon, J. G. II. *J. Electochem. Soc.* **1990**, *137*, 2672-2677.
7. Pourbaix, M. *Atlas of Electrochemical Equilibria in Aqueous Solutions*, Pergamon Press, New York, 1966.
8. Strehblow, H.-H.; Titze, B. *Electrochim. Acta* **1980**, *25*, 839-850.
9. Abrantes, L. M.; Castillo, L. M.; Norman, C.; Peter, L. M. *J. Electroanal. Chem.* **1984**, *163*, 209-221.
10. Boukamp, B. A. *EQUIVCRT Software Manual*, University of Twente, Enschede, The Netherlands, 1993.
11. Gabrielli, C. *Identification of Electrochemical Processes by Frequency Response Analysis*, Technical Report Number 004/83, Solartron Instruments, England.
12. "Applications of impedance spectroscopy." In *Impedance Spectroscopy, Theory, Experiments and Applications*; Barsoukov, E.; MacDonald, J. R., Eds.; John Wiley and Sons, New York, 2005.
13. Chan, H. Y. H.; Takoudis, C. G.; Weaver, M. J. *J. Phys. Chem.* **1999**, *B103*, 357-365.
14. Walter, G. W. *J. Electroanal. Chem.* **1981**, *118*, 259-273.
15. Muralidheren, V. S. *Anti-Corrosion Methods and Materials* **1997**, *44*, 26-29.
16. Omanovic, S.; Metikos-Hukovic, M. *Thin Solid Films* **1995**, *266*, 31-37.
17. Chao, C. Y.; Lin, L. F.; Macdonald, D. D. *J. Electrochem. Soc.* **1981**, *128*, 1187-1194.
18. Macdonald, D. D.; Ben-Haim, M.; Pallix, J. *J. Electrochem. Soc.* **1989**, *136*, 3269-3273.